View metadata, citation and similar papers at core.ac.uk

brought to you by CORE

provided by Institutional Research Information System University of Turin

UNIVERSITÀ DEGLI STUDI DI TORINO

This is an author version of the contribution published on:

Lanzardo S, Conti L, Rooke R, Ruiu R, Accart N, Bolli E, Arigoni M, Macagno M, Barrera G, Pizzimenti S, Aurisicchio L, Calogero RA, Cavallo F

Immunotargeting of Antigen xCT Attenuates Stem-like Cell Behavior and Metastatic Progression in Breast Cancer.

In Cancer Res. 2016 Jan 1;76(1):62-72

The definitive version is available at:

DOI: 10.1158/0008-5472.CAN-15-1208

Immunotargeting of antigen xCT attenuates stem-like cell behavior and metastatic progression in breast cancer

Stefania Lanzardo[1]*, Laura Conti[1]*, Ronald Rooke[2], Roberto Ruiu[1], Nathalie Accart[3], Elisabetta Bolli[1], Maddalena Arigoni[1], Marco Macagno[1], Giuseppina Barrera[4], Stefania Pizzimenti[4], Luigi Aurisicchio[5], Raffaele Adolfo Calogero[1], Federica Cavallo[1].

[1]Department of Molecular Biotechnology and Health Sciences, Molecular Biotechnology Center, University of Turin, Turin, Italy; [2]Elsalys Biotech, Illkirch Graffenstaden, 67400, France; [3]Novartis Institute for medical research, CH-4002, Basel, Switzerland; [4]Department of Clinical and Biological Sciences, University of Turin, Turin, Italy; [5]Takis, Via di Castel Romano, Rome, Italy.

*These authors contributed equally to this work

Running title: anti-xCT vaccination for Cancer Stem Cell targeting

Keywords

Cancer Stem Cells; breast cancer; cancer immunotherapy; DNA vaccination; xCT.

Financial support

This work has been supported with grants from the Italian Association for Cancer Research (IG 11675), Fondazione Ricerca Molinette Onlus, the University of Turin and the Compagnia di San Paolo (Progetti di Ricerca Ateneo/CSP). L.C. has been supported with a fellowships from the Fondazione Umberto Veronesi, "Pink is Good" project.

Corresponding Author: Federica Cavallo, Molecular Biotechnology Center, Via Nizza 52, 10126 Turin, Italy. Phone: +39-011-6706457; Fax: +39-011-2365417; E-mail: federica.cavallo@unito.it

Disclosure of Potential Conflicts of Interest: no potential conflicts of interest exist.

Total word count: 4998

Total number of figures: 6

Abstract

Resistance to therapy and lack of curative treatments for metastatic breast cancer suggest that current therapies may be missing the subpopulation of chemo- and radio-resistant cancer stem cells (CSC). The ultimate success of any treatment may well rest on CSC eradication, but specific anti-CSC therapies are still limited. A comparison of the transcriptional profiles of murine Her2+ breast tumor TUBO cells and their derived CSC-enriched tumorspheres has identified xCT, the functional subunit of the cystine/glutamate antiporter system xc-, as a surface protein that is upregulated specifically in tumorspheres. We validated this finding by cytofluorimetric analysis and immunofluorescence in TUBO-derived tumorspheres and in a panel of mouse and human triple negative breast cancer (TNBC) cell-derived tumorspheres. We further show that downregulation of xCT impaired tumorsphere generation and altered CSC intracellular redox balance in vitro, suggesting that xCT plays a functional role in CSC biology. DNA vaccination-based immunotargeting of xCT in mice challenged with syngeneic tumorsphere-derived cells delayed established subcutaneous tumor growth and strongly impaired pulmonary metastasis formation by generating anti-xCT antibodies able to alter CSC self-renewal and redox balance. Finally, anti-xCT vaccination increased CSC chemosensitivity to doxorubicin in vivo, indicating that xCT immunotargeting may be an effective adjuvant to chemotherapy.

Precis

Immunotargeting of breast cancer stem-like cells can sensitize them to chemotherapy, offering an effective strategy to overcome drug resistance and limit metastatic progression.

Introduction

Despite recent advances in breast cancer management resulting in a decrease in overall mortality (1), minimal residual disease and local and distant post-treatment recurrences are still major obstacles to complete remission. According to the cancer stem cell (CSC) model, these residual elements are caused by a stem-like subpopulation of tumor cells that are endowed with self-renewal and multi-lineage differentiation capabilities, chemo- and radio-resistance and the ability to give metastases (2). The therapeutic implication of CSC model is that a tumor needs to be deprived of its CSC population to be completely eradicated. Novel anticancer strategies must therefore be developed to face this new challenge.

Active immunotherapy, i.e. vaccination, is an attractive approach to target CSC. Preclinical studies have shown that CSC are immunogenic and a more effective antigen source for inducing protective anti-tumor immunity in mice than unselected tumor cells (3). Several clinical trials in which CSC lysate or mRNA are used to pulse or transfect autologous dendritic cells (DC), that are then injected back into the patients, are currently underway in various tumor settings (4). However, this technique presents the difficulty of setting up standardized functional DC production procedures (5). A promising alternative can be found in powerful and versatile DNA-based vaccines which combines lower manufacturing costs and more standardized production processes while also inducing strong immunological responses against tumor antigens. Nevertheless, one must identify a suitable target to develop a DNA-based vaccine; as no consensus on the expression of specific vaccination targets by CSC currently exists, pre-clinical screening by high-throughput technologies can be of use in uncovering antigens for CSC-targeted genetic vaccines.

We have compared the transcription profile of the murine $Her2^+$ breast cancer TUBO cell line (6) with that of its CSC-enriched tumorspheres in order to identify antigens expressed by mammary CSC. Among the genes upregulated in tumorspheres and associated with poor prognosis in several datasets of human mammary cancer, we focused on xCT. It is the light chain of the antiporter system x_c^-, which imports the aminoacid cystine into cells in exchange with glutamate. Cystine is the rate-limiting substrate for the synthesis of the antioxidant glutathione (GSH), which is known to be involved in the detoxification of reactive oxygen species (ROS) (7).

xCT is highly expressed by a variety of malignant tumors (7-12) and plays an important role in cancer growth, progression, metastatic dissemination (13-15) and drug resistance (16). Moreover, its membrane expression is stabilized via direct interaction with a CD44 variant (13), while targeting xCT has been found to deplete undifferentiated CD44v-expressing cancer cells in a xenografted model of head and neck squamous cell carcinoma, sensitizing the tumor to other therapies (17).

We herein report that xCT upregulation is a general feature of breast CSC and that plays a functional role in CSC biology and intracellular redox balance. We demonstrate that anti-xCT DNA vaccination slows established subcutaneous tumor growth, efficiently impairs lung metastasis formation and increases CSC chemosensitivity, thus making it a novel therapeutic approach for breast cancer treatment.

Materials and Methods

Cell and tumorsphere cultures

MDA-MB-231, HCC-1806 and 4T1 cells were purchased from ATCC (LGC Standards) and cultured as in (18). NIH/3T3 cells were cultured as in (19). Cells were passaged in our laboratory for fewer than six months after their resuscitation. TUBO cells and tumorspheres were generated as in (18). Human cell lines were tested utilizing Short Tandem Repeat (STR) profiling.

FACS analysis

Cells and tumorspheres were stained with AlexaFluor647-anti-Sca-1, PE-anti-CD44 and PE/Cy7-anti-CD24 (Biolegend), and with goat anti-xCT (Santa Cruz Biotechnology) antibodies followed by rabbit FITC-anti-goat Ig (Dako), or with Aldefluor kit (StemCell Technologies), as in (18). To quantify anti-xCT antibody titers, tumorsphere-derived and NIH/3T3 cells were incubated with sera of vaccinated mice and subsequently with rabbit FITC-anti-mouse Ig (Dako). Cells were stained with 2',7'-dihydrochlorofluorescein diacetate (DHCF-DA, Sigma-Aldrich) as in (20). All samples were analyzed on a CyAnADP Flow Cytometer, using Summit 4.3 software (Beckman Coulter).

Fluorescent microscopy

Tumor microarrays (TMA) (Biochain # T8234700-2, lot # B406087, and Biochain # T6235086-5, lot # B112136) of normal or tumor human tissues were blocked in 3%H_2O_2 (Sigma-Aldrich), followed by 1%BSA, and then incubated with anti-xCT or isotype-matched control antibodies (Abcam). The signal was amplified as in (21) and sections were fixed in 1%formaldehyde (Sigma-Aldrich), counterstained with DAPI (Sigma-Aldrich) and mounted in Mowiol® (Calbiochem). Images were acquired using a confocal microscope LSM700 and Zen software 7.0.0.285 (Zeiss). Slides were scanned on a slide scanner (Hamamatsu Nanozoomer 2.0RS) using the Calopix software. xCT^+ cell percentage was defined by quantifying blue (nuclei) and red (xCT) surface areas and calculated as the ratio of xCT expression (i.e. xCT stained surface/xCT+nuclei surface).

Tumorspheres were cytospinned to glass slides, fixed in 4%formaldehyde and then incubated with rabbit anti-OCT4 (Abcam), rat PE-anti-Sca-1 (Santa Cruz biotechnology), mouse APC/eFluor780-anti-Thy1.1

(eBioscience) or the matched isotype control antibodies. Cytospinned tumorspheres or NIH/3T3 cultured on glass coverslips were stained with IgG purified from immunized mice sera and then with rabbit AlexaFluor488-anti-mouse or goat Texas red-anti-rabbit secondary antibodies (Life Technologies). Images were acquired on ApoTome system and AxioVision Release4.8 software (Zeiss).

In vitro cytotoxicity

24 hours after TUBO cells and tumorspheres seeding in 96-well plates, scalar doses of doxorubicin or sulfasalazine (SASP) (Sigma-Aldrich) were added and incubated at 37°C for 72 hours. Cytotoxicity was evaluated with MTT using the Cell Proliferation Kit I (Roche Diagnostics).

RNA interference

xCT downregulation in tumorspheres was performed using a pool of specific siRNAs, or scrambled siRNAs (Invitrogen Corp.), as in (18).

SASP effects on tumorsphere formation

Dissociated tumorspheres were cultured with scalar doses of SASP or its diluent DMSO (Sigma-Aldrich), and the total number of tumorspheres/well was counted 5 days later.

Measurement of ROS and GSH

ROS amount was analyzed as 2',7'-dichlorofluorescin (DCF) formation in cells incubated with 5μM DHCF-DA for 20 minutes at 37°C using the Luminescence Spectrometer LS 55 (Perkin–Elmer), quantified using a DCF standard curve and expressed as pmol DCF formed/min/mg protein (22). GSH content was assessed by determining non-protein sulphydryl content, as in (23), and calculated using a GSH standard curve. Results are expressed as μg GSH/mg of cellular proteins.

Plasmids

The cDNA sequence for mouse xCT (NM_011990.2), in the pDream2.1 plasmid (GenScript), was cloned in a pVAX1 (Invitrogen) plasmid (pVAX1-xCT), sequenced (BMR Genomics), and produced with EndoFree Plasmid Giga kits (Qiagen Inc.).

Immune sera effect on tumorsphere formation

Serum IgG from vaccinated mice were purified using the Melon Gel purification kit (Thermo Scientific) and incubated with tumorsphere-derived cells. After 5 days, spheres were counted and analyzed for CSC markers expression and ROS production by FACS.

In Vivo Treatments

Wild type (Charles River Laboratories) and Ig μ-chain gene knocked out (BALB-μIgKO) (24) BALB/c mice were maintained at the Molecular Biotechnology Center, University of Torino, and treated in accordance with University Ethical Committee and European guidelines under Directive 2010/63. Vaccination, performed either before or after tumor challenge, consisted of two i.m. electroporation at two weeks interval, of pVAX1 or pVAX1-xCT plasmids as previously described (25).

Primary s.c. tumors were induced by injecting $1x10^4$ TUBO or 4T1 tumorsphere-derived cells. Some tumors were explanted and tumorspheres generated as in (26). Lung metastases were induced either by injecting i.v. $5x10^4$ TUBO tumorsphere-derived cells or by injecting s.c. $1x10^4$ 4T1 tumorsphere-derived cells. In the latter case, lungs were removed when s.c. tumors reached 10 mm mean diameter. Micrometastases were counted on a Nikon SMZ1000 stereomicroscope (Mager Scientific).

Doxorubicin treatment consisted of the i.v. administration of a total dose of 10 mg/Kg either in a single injection or in two administration at a week interval.

Statistical analysis

Differences in latency, sphere formation, protein expression, GSH and ROS levels and metastasis number were evaluated using a Student's *t*-test. Data are shown as the mean ± SEM unless otherwise stated. Values of $P < 0,05$ were considered significant.

xCT is upregulated in breast CSC

To identify the transcripts associated with mouse and human mammary CSC, we compared the transcription profile of $Her2^+$ murine TUBO cells which had been cultured as an epithelial monolayer, with the profiles of the first three *in vitro* passages of their derived tumorspheres (P1, P2 and P3) using MouseWG-6 v2.0 Illumina beadchips (GSE21451) (Supplementary Figure 1A). This analysis uncovered a cluster of transcripts whose expression rose, as well as three clusters whose expression decreased from TUBO through P1 to P3 cells (Supplementary Figure 1B).

We devised a ranking procedure according to the clinical outcome (CO) of tumors expressing the transcripts that we found increased in tumorspheres (27), using data from six public human breast cancer datasets (see Supplementary methods). One of the genes with the best CO score was xCT (7) (Slc7a11, Supplementary Figure 1C), whose expression increased progressively from TUBO to P3 tumorspheres, as confirmed by FACS (Figure 1A) and qPCR (Supplementary Figure 2) analyses. Interestingly, most P3-derived cells that express the stem cell marker Sca-1 (26) are also xCT^+ (Figure 1B). The immunofluorescence analysis revealed widespread xCT positivity in tumorspheres that are essentially composed of CSC, as confirmed by Sca-1, OCT4 and Thy1.1 marker expression patterns (Figure 1C). xCT upregulation is a feature of breast CSC and is not due to tumorsphere culture conditions, since it was also observed on the small $CD44^{high}CD24^{low}$ CSC population present in TUBO cells (Figure 1D). Moreover, xCT upregulationis not restricted to TUBO-derived CSC as it was also observed in tumorspheres derived from mouse (4T1) and human (HCC-1806 and MDA-MB-231) TNBC cell lines (Figure 1E), suggesting that xCT may be a hallmark of breast cancer CSC.

xCT expression in the TMA of normal and neoplastic samples was evaluated to address its distribution in human cancers. xCT expression was low in normal mammary glands (Figure 1F, left panel) as it was in the other normal tissues tested (Supplementary Figure 3A). By contrast, xCT was expressed at high levels in many neoplastic tissues (Supplementary Figure 3B), including hyperplastic mammary lesions and invasive ductal breast carcinomas (IDC) (Figure 1F, middle and right panels) displaying a pattern in which it is confined to neoplastic cells. In particular, we found xCT expression in 62% of $Her2^+$, 57% of estrogen/progesterone

receptor^{+} Her2^{-} (ER/PR^{+}Her2^{-}), and 35% of TNBC samples (Figure 1G), suggesting that xCT may well be a commonly upregulated target in breast cancers.

xCT downregulation impairs tumorsphere generation and alters intracellular redox balance

A MTT test was performed on TUBO cells and tumorspheres that had either been treated or not with scalar doses of xCT inhibitor SASP (28). While SASP did not decrease TUBO cell viability, except for the highest dose (100 μM; IC_{50} 126,1 ± 25,7 μM; Figure 2A), tumorsphere viability was inhibited in a dose dependent manner (IC_{50} 51,6 ± 3,5 μM; Figure 2B), suggesting that CSC are sensitive to xCT inhibition. Similarly, xCT silencing through a pool of specific siRNAs impaired tumorspheres but not TUBO cell viability (Figures 2A, B). Moreover, SASP treatment and xCT silencing impaired tumorsphere generation (Figure 2C, D). FACS analyses performed 24 hours after siRNA transfection showed that the reduction in xCT^{+} cells (Figure 2E, F) is accompanied by a reduction in CSC, i.e. Sca1^{+} and CD44$^{high/}$CD24^{low} cells (Figure 2F). On the contrary, xCT overexpression increases colony generating ability, as confirmed by the higher number of colonies generated in soft agar by NIH/3T3 and HEK-293 cells transfected with xCT when compared to the corresponding cells transfected with empty plasmids (Supplementary Figure 4). Taken together, these data suggest that xCT plays an important role in CSC maintenance and sphere generation.

As xCT is an important determinant of redox balance (13), we evaluated GSH and ROS levels in TUBO cells and tumorspheres. GSH amount was significantly greater in tumorspheres than in TUBO cells (Figure 2G), whereas ROS levels were lower (Figure 2H). xCT downregulation caused a significant decrease in GSH and an increase in ROS levels (Figure 2G, H) as compared to controls, suggesting that CSC have a higher ROS defense capability than epithelial tumor cells.

Anti-xCT vaccination induces antibodies that inhibit CSC

BALB/c mice were vaccinated with either pVAX1-xCT or pVAX1 to evaluate whether xCT is a potential target for cancer immunotherapy. No T-cell response was observed against the H-2K^{d} dominant mouse xCT peptide (Supplementary Figure 5A, B). Tumorsphere-derived cells were stained with the sera of vaccinated mice to

evaluate their humoral response, and specific antibody binding was analyzed by FACS. pVAX1-xCT vaccination induced the production of CSC-binding antibodies, which were not detectable in empty pVAX1 vaccinated mouse sera (Figure 3A-C). These results were confirmed by the ability of purified IgG, from pVAX1-xCT vaccinated mouse sera, to stain tumorspheres (Figure 3D). These antibodies are specific for xCT, since no binding was observed in NIH/3T3 cells negative for xCT expression (Figure 3E-H).

Of note, TUBO cells incubated with IgG purified from pVAX1-xCT vaccinated mice displayed reduced sphere-generation ability (Figure 3I), a lower percentage of stem cell marker positive cells (Figure 3L), but increased ROS content as compared to control IgG (Figure 3M).

These results suggest that anti-xCT vaccination induces antibodies targeting xCT, thus affecting self-renewal and ROS production in CSC.

Anti-xCT vaccination slows *in vivo* breast tumor growth

TUBO-derived tumorspheres were s.c. implanted into BALB/c mice that were vaccinated when tumors reached 2 or 4 mm mean diameter to evaluate whether xCT immune-targeting hinders breast cancer growth (Figure 4A-D). Tumors grew progressively in the pVAX1 group of 2 mm vaccinated mice (Figure 4A), while tumors regressed in 23,8% of pVAX1-xCT vaccinated mice (Figure 4B). Tumor growth kinetics were slower in the latter group than in the pVAX1 group, as proven by the significantly shorter time required for tumors to reach 4 or 6 mm mean diameter (20.7±2,7 and 30.7±3,6 days in pVAX1-mxCT vaccinated mice versus 12.9±2 and 20.8±2,5 days in control mice). Anti-xCT vaccination also induced tumor regression in 16% of mice that were treated when their tumors measured 4 mm mean diameter (Figure 4D), while all tumors in the pVAX1 group reached 10 mm mean diameter in less than 60 days (Figure 4C). The efficacy of anti-xCT vaccination was then evaluated against 2 or 4 mm mean diameter tumors obtained when 4T1 tumorsphere derived-cells were injected s.c. (Figure 4E-H). In 2 mm tumor vaccinated mice, tumors grew rapidly in pVAX1 group (Figure 4E), while tumor growth kinetics were generally slower and the time required for the tumors to reach 4, 6, 8 or 10 mm mean diameter was significantly longer in the pVAX1-xCT vaccinated group (10.4±1.3; 15.6±1.6; 20.4±1.3; 23.4±1.2 days in pVAX1-xCT vaccinated mice versus 4.9±0.5; 10±1.1; 14.6±1.0; 17.4±0.8 days in control

mice). Similarly, the 4 mm tumor vaccinated group displayed slower tumor growth in pVAX1-xCT vaccinated mice (Figure 4E, H), and the time required for the tumors to reach 6, 8 or 10 mm mean diameter was significantly longer (9.2±0.9; 13.1±0.9; 17.0±0.5 days in pVAX1-xCT vaccinated mice versus 5.2±0.9; 8.8±1.0; 13.0±1.6 days in control mice), indicating that xCT immunotherapy may be beneficial in various breast cancer subtypes.

Tumor remission in vaccinated mice might be due to a reduction of CSC frequency as a consequence of the treatment, as suggested by the decrease in the percentage of Aldefluor^{+} cells in regressing tumors from mice vaccinated with pVAX1-xCT plasmid (Figure 4I). Moreover, the cells composing the tumor mass had a significantly decreased tumorsphere forming ability (Figure 4L) when compared with cells derived from tumors grown in pVAX1 vaccinated mice.

Anti-xCT vaccination prevents lung metastasis formation

BALB/c mice were vaccinated with pVAX1 or pVAX1-xCT plasmids and i.v. injected with TUBO-derived tumorspheres to evaluate the effects of anti-xCT vaccination on lung metastasis formation. Metastasis number was significantly reduced after pVAX1-xCT vaccination, as reported in Figures 5A and B. This anti-metastatic effect is dependent on the specific antibodies elicited by anti-xCT vaccination, since no effect was observed vaccinating BALB-μIgKO mice i.v. injected with TUBO-derived tumorspheres (Figures 5C, D).

Anti-xCT vaccination was also able to reduce the number of spontaneous metastases generated from the s.c. injection of 4T1-derived tumorspheres, either when vaccination was performed before tumorspheres injection (Figure 5E, F) or when mice already had a 2 mm mean diameter tumor (Figure 5G, H).

Altogether, these findings suggest that anti-xCT vaccination interferes with CSC metastatic properties both in a preventive and therapeutic setting. This anti-metastatic activity is due to CSC immunotargeting, since no effect was observed in xCT-vaccinated mice injected with differentiated tumor cells (Supplementary Figure 6A, B) or in mice vaccinated against Her3 (29) and injected with TUBO-derived tumorspheres (Supplementary Figure 7 A-F). In this model Her3 is not a CSC-specific antigen, since it is equally expressed on TUBO cells and tumorspheres.

Anti-xCT vaccination enhances the effect of doxorubicin

In accordance with CSC resistance to chemotherapy (2), TUBO cells display a higher sensitivity to doxorubicin than tumorspheres (Figure 6A, B). Since xCT is involved in maintaining the intracellular redox balance, thus counteracting the effects of ROS-generating cytotoxic drugs (13), it is likely that targeting xCT could increase CSC chemosensitivity. In order to explore this hypothesis *in vivo*, unvaccinated, pVAX1-xCT and pVAX1 vaccinated mice were i.v. injected with TUBO-derived tumorspheres and either treated with doxorubicin or not. As shown in Figure 6C, pVAX1-xCT determined a decrease in the number of lung metastases compared to the control and doxorubicin treated mice and the combination of vaccination and doxorubicin significantly improved the activity of individual treatments.

Similar results were observed in mice challenged with s.c. injection of TUBO-derived tumorspheres and subjected to vaccination and chemotherapy when tumors reached 2 mm mean diameter. The tumor regressed in 25% of mice treated with doxorubicin alone (Figure 6D) or in combination with pVAX1 plasmid (Figure 6E), while the combination of doxorubicin and anti-xCT vaccination stopped tumor progression in 60% mice (Figure 6F).

All together, these data suggest that anti-xCT vaccination may well be an efficient adjuvant treatment for chemotherapy both in a preventive and in a therapeutic setting.

Discussion

A key challenge in anticancer therapy is the development of treatments able to both shrink a tumor and kill CSC, which are resistant to current chemo- and radio-therapies, and are considered the source of tumor recurrence and metastatic spread. However, the identification of ideal CSC-associated targets is a particularly tough task since CSC appear to be "moving targets" that switch between different cell states during cancer progression (30). Hence, antigens that are upregulated in CSC but also present in more differentiated cancer cells would appear to be outstanding candidates.

A possible candidate with these features is xCT, that we have identified as upregulated in breast $Her2^{+}$ and TNBC CSC. Importantly, its expression is not confined to CSC, since we were able to detect its presence on cancer cells in human hyperplastic mammary glands as well as in IDC, independently from their histological subtype. xCT possesses all the features of an ideal target for immunotherapy against undifferentiated and more differentiated cancer cells. This speculation is strengthened by our meta-analyses, performed on human breast cancer datasets, that link high xCT expression to poor prognosis.

Moreover, xCT expression is not limited to breast cancer. Our analyses, performed on a plethora of healthy and neoplastic tissues, and data obtained elsewhere in other tumors (7,31,32) have identified xCT as a distinctive cancer marker and suggested that its targeting may be of benefit in the treatment of a wide range of neoplastic diseases.

Another important feature of xCT as immunotherapy target is its functional role, which becomes essential in CSC. Indeed, the impairment of sphere-generation following the pharmacological or genetic downregulation of xCT reflects the role of this protein in the regulation of CSC self-renewal, indicating that xCT is not a simple bystander of the stem-like phenotype in breast cancer, but that it also plays a role in CSC biology.

xCT function in CSC self-renewal might be mediated by the regulation of the mechanisms that govern CSC intracellular redox balance. Although further studies are needed to better define this mechanism in our model, it has been shown that intracellular ROS concentration can affect CSC viability and self-renewal (33-35). CSC upregulate the key regulator of the anti-oxidant response Nuclear factor erythroid 2-related factor 2 (36) and

many anti-oxidant enzymes, such as superoxide dismutase 2, glutathione peroxidases and heme oxygenase 1, that attempt to maintain intracellular ROS at levels lower than those observed in differentiated cancer cells (37). In accordance with this, a basal increase in GSH and decrease in ROS levels were observed in tumorspheres as compared to TUBO cells, which can be explained by xCT upregulation in tumorspheres and proven by the fact that xCT downregulation reverts this phenotype.

Several authors have advocated the use of xCT as a therapeutic target for pharmacological inhibition using the administration of SASP, a FDA-approved, anti-inflammatory drug for the treatment of inflammatory bowel disease, ulcerative colitis and Crohn's disease (38). However, SASP exerts many effects in addition to its ability to interfere with xCT function, so it cannot be considered a specific xCT inhibitor (39). Although recent preclinical models demonstrated that SASP impairs cancer growth and metastatic spread via xCT inhibition (15,17,40), its use in cancer patients is hampered by its low specificity, short bio-availability and numerous side effects (41).

We have chosen DNA-based antitumor vaccination as our xCT targeting option on the basis of our consolidated expertise in the field and the considerations stated above. In fact, DNA vaccination is a cost-effective technology able to induce a significant immune activation against tumor antigens in a specific and well tolerated way, thus reducing off-target effects (42). This paper sees the first report of xCT being targeted with a DNA-based vaccination strategy that efficiently slows mammary tumor growth and prevents lung metastasis formation. Our data show that, despite xCT being a self-antigen, DNA vaccination is able to induce an antibody-based immune response against the tumor; a lack of T-cell response against xCT may be caused by a thymic depletion of high-avidity T-cell clones, as we have previously reported for the Her2 antigen in the BALB-neuT model (43). Notably, the anti-tumor effects were lost in B cell deficient mice, confirming the central role of vaccine-induced antibodies. The anti-tumor effects observed *in vivo* may result from the CSC self-renewal and redox balance impairment induced by anti-xCT antibodies, as indicated by our *in vitro* observations. This is particularly evident in the inhibition of lung metastasis formation, most likely because CSC self-renewal is essential for re-initiating growth at the metastatic site (44).

Interestingly, we were not able to detect any vaccine side effect as xCT expression in normal tissues is almost completely limited to the brain, which can barley be reached by circulating antibodies by virtue of the blood-brain barrier (45). However, it has been reported that xCT may also regulate immune cell functions. In fact, xCT mediates cystine uptake in macrophages and dendritic cells, which are the only source of free cysteine release which, in turn, is essential for the antigen-driven activation of T lymphocytes (46). However, by vaccinating mice against both xCT and Her2, we observed that xCT targeting does not impair the Her2 specific T cell response (Supplementary Figure 5C, D). The safety of xCT immune targeting is further sustained by the fact that its genetic ablation in mice does not alter vital biological functions (47).

xCT participate in cancer cells' resistance to a variety of antitumor drugs (16). Its action here is thought to be linked to its role in intracellular redox balance, as many chemotherapeutic drugs exert their function, at least in part, by increasing oxidative stress (48). It is worth noting that tumorspheres display significantly increased resistance to doxorubicin, a drug largely used in breast cancer therapy, as compared to epithelial TUBO cells. This fits with the observation that CSC are chemoresistant (2), and may reflect the increased expression of xCT in tumorspheres. In this regard, it has been demonstrated that xCT inhibition promotes the sensitization of tumor cells to doxorubicin (49,50). In accordance with these findings, we have observed that a combination of anti-xCT vaccination and doxorubicin strongly enhanced the anti-metastatic potential of the individual treatments. This observation strengthens the translatability of this immunotherapeutic approach to clinical trials, where new experimental protocols are routinely tested in combination with standard treatments.

In conclusion, we have shown for the first time that xCT immunotargeting is effective in impairing tumor growth and metastasis formation *in vivo*. We propose a mechanism by which anti-xCT vaccination exerts its anti-neoplastic function across two separate, but complementary, fronts: i) a direct effect on CSC through immune-mediated eradication and ii) inhibition of xCT function on CSC, leading to impairment of tumorigenic and stem-like properties and their sensitizing to chemotherapy. Moreover, a possible additional anti-cancer mechanism may occur, by which the anti-xCT antibodies induced by vaccination may suppress the myeloid

346 derived suppressor cells that exploit xCT for their inhibitory activity (46). However, this hypothesis is still to be
347 verified.
348 Further studies will thoroughly investigate the interactions between chemotherapy and anti-xCT vaccination and
349 all possible side effects in order to accelerate translation to the clinic, as a safe tool to combat CSC with in
350 patients is sorely needed.

References

1. Siegel R, DeSantis C, Virgo K, Stein K, Mariotto A, Smith T, et al. Cancer treatment and survivorship statistics, 2012. CA Cancer J Clin 2012;62(4):220-41.
2. Frank NY, Schatton T, Frank MH. The therapeutic promise of the cancer stem cell concept. The Journal of clinical investigation 2010;120(1):41-50.
3. Ning N, Pan Q, Zheng F, Teitz-Tennenbaum S, Egenti M, Yet J, et al. Cancer stem cell vaccination confers significant antitumor immunity. Cancer research 2012;72(7):1853-64.
4. Kwiatkowska-Borowczyk EP, Gabka-Buszek A, Jankowski J, Mackiewicz A. Immunotargeting of cancer stem cells. Contemporary oncology 2015;19(1A):A52-9.
5. Aurisicchio L, Ciliberto G. Genetic cancer vaccines: current status and perspectives. Expert Opin Biol Ther 2012;12(8):1043-58.
6. Rovero S, Amici A, Di Carlo E, Bei R, Nanni P, Quaglino E, et al. DNA vaccination against rat her-2/Neu p185 more effectively inhibits carcinogenesis than transplantable carcinomas in transgenic BALB/c mice. J Immunol 2000;165(9):5133-42.
7. Lewerenz J, Hewett SJ, Huang Y, Lambros M, Gout PW, Kalivas PW, et al. The cystine/glutamate antiporter system x(c)(-) in health and disease: from molecular mechanisms to novel therapeutic opportunities. Antioxid Redox Signal 2013;18(5):522-55.
8. Gout PW, Buckley AR, Simms CR, Bruchovsky N. Sulfasalazine, a potent suppressor of lymphoma growth by inhibition of the x(c)- cystine transporter: a new action for an old drug. Leukemia 2001;15(10):1633-40.
9. Chung WJ, Lyons SA, Nelson GM, Hamza H, Gladson CL, Gillespie GY, et al. Inhibition of cystine uptake disrupts the growth of primary brain tumors. J Neurosci 2005;25(31):7101-10.
10. Narang VS, Pauletti GM, Gout PW, Buckley DJ, Buckley AR. Suppression of cystine uptake by sulfasalazine inhibits proliferation of human mammary carcinoma cells. Anticancer Res 2003;23(6C):4571-9.
11. Doxsee DW, Gout PW, Kurita T, Lo M, Buckley AR, Wang Y, et al. Sulfasalazine-induced cystine starvation: potential use for prostate cancer therapy. Prostate 2007;67(2):162-71.
12. Jiang L, Kon N, Li T, Wang SJ, Su T, Hibshoosh H, et al. Ferroptosis as a p53-mediated activity during tumour suppression. Nature 2015;520(7545):57-62.
13. Ishimoto T, Nagano O, Yae T, Tamada M, Motohara T, Oshima H, et al. CD44 variant regulates redox status in cancer cells by stabilizing the xCT subunit of system xc(-) and thereby promotes tumor growth. Cancer cell 2011;19(3):387-400.
14. Timmerman LA, Holton T, Yuneva M, Louie RJ, Padro M, Daemen A, et al. Glutamine sensitivity analysis identifies the xCT antiporter as a common triple-negative breast tumor therapeutic target. Cancer cell 2013;24(4):450-65.
15. Chen RS, Song YM, Zhou ZY, Tong T, Li Y, Fu M, et al. Disruption of xCT inhibits cancer cell metastasis via the caveolin-1/beta-catenin pathway. Oncogene 2009;28(4):599-609.
16. Huang Y, Dai Z, Barbacioru C, Sadee W. Cystine-glutamate transporter SLC7A11 in cancer chemosensitivity and chemoresistance. Cancer Res 2005;65(16):7446-54.
17. Yoshikawa M, Tsuchihashi K, Ishimoto T, Yae T, Motohara T, Sugihara E, et al. xCT inhibition depletes CD44v-expressing tumor cells that are resistant to EGFR-targeted therapy in head and neck squamous cell carcinoma. Cancer Res 2013;73(6):1855-66.
18. Conti L, Lanzardo S, Arigoni M, Antonazzo R, Radaelli E, Cantarella D, et al. The noninflammatory role of high mobility group box 1/Toll-like receptor 2 axis in the self-renewal of mammary cancer stem cells. FASEB J 2013;27(12):4731-44.
19. Quaglino E, Mastini C, Amici A, Marchini C, Iezzi M, Lanzardo S, et al. A better immune reaction to Erbb-2 tumors is elicited in mice by DNA vaccines encoding rat/human chimeric proteins. Cancer Res 2010;70(7):2604-12.
20. Donato MT, Martinez-Romero A, Jimenez N, Negro A, Herrera G, Castell JV, et al. Cytometric analysis for drug-induced steatosis in HepG2 cells. Chem Biol Interact 2009;181(3):417-23.
21. Fend L, Accart N, Kintz J, Cochin S, Reymann C, Le Pogam F, et al. Therapeutic effects of anti-CD115 monoclonal antibody in mouse cancer models through dual inhibition of tumor-associated macrophages and osteoclasts. PLoS One 2013;8(9):e73310.

22. Ravindranath V. Animal models and molecular markers for cerebral ischemia-reperfusion injury in brain. Methods Enzymol 1994;233:610-9.
23. Sedlak J, Lindsay RH. Estimation of total, protein-bound, and nonprotein sulfhydryl groups in tissue with Ellman's reagent. Anal Biochem 1968;25(1):192-205.
24. Nanni P, Landuzzi L, Nicoletti G, De Giovanni C, Rossi I, Croci S, et al. Immunoprevention of mammary carcinoma in HER-2/neu transgenic mice is IFN-gamma and B cell dependent. J Immunol 2004;173(4):2288-96.
25. Arigoni M, Barutello G, Lanzardo S, Longo D, Aime S, Curcio C, et al. A vaccine targeting angiomotin induces an antibody response which alters tumor vessel permeability and hampers the growth of established tumors. Angiogenesis 2012;15(2):305-16.
26. Grange C, Lanzardo S, Cavallo F, Camussi G, Bussolati B. Sca-1 identifies the tumor-initiating cells in mammary tumors of BALB-neuT transgenic mice. Neoplasia 2008;10(12):1433-43.
27. Riccardo F, Arigoni M, Buson G, Zago E, Iezzi M, Longo D, et al. Characterization of a genetic mouse model of lung cancer: a promise to identify Non-Small Cell Lung Cancer therapeutic targets and biomarkers. BMC genomics 2014;15 Suppl 3:S1.
28. Lo M, Wang YZ, Gout PW. The x(c)- cystine/glutamate antiporter: a potential target for therapy of cancer and other diseases. J Cell Physiol 2008;215(3):593-602.
29. Sithanandam G, Anderson LM. The ERBB3 receptor in cancer and cancer gene therapy. Cancer Gene Ther 2008;15(7):413-48.
30. Schwitalla S. Tumor cell plasticity: the challenge to catch a moving target. J Gastroenterol 2014;49(4):618-27.
31. Kinoshita H, Okabe H, Beppu T, Chikamoto A, Hayashi H, Imai K, et al. Cystine/glutamic acid transporter is a novel marker for predicting poor survival in patients with hepatocellular carcinoma. Oncol Rep 2013;29(2):685-9.
32. Sugano K, Maeda K, Ohtani H, Nagahara H, Shibutani M, Hirakawa K. Expression of xCT as a predictor of disease recurrence in patients with colorectal cancer. Anticancer Res 2015;35(2):677-82.
33. Singer E, Judkins J, Salomonis N, Matlaf L, Soteropoulos P, McAllister S, et al. Reactive oxygen species-mediated therapeutic response and resistance in glioblastoma. Cell Death Dis 2015;6:e1601.
34. Sato A, Okada M, Shibuya K, Watanabe E, Seino S, Narita Y, et al. Pivotal role for ROS activation of p38 MAPK in the control of differentiation and tumor-initiating capacity of glioma-initiating cells. Stem Cell Res 2014;12(1):119-31.
35. Shi X, Zhang Y, Zheng J, Pan J. Reactive oxygen species in cancer stem cells. Antioxid Redox Signal 2012;16(11):1215-28.
36. Ryoo IG, Choi BH, Kwak MK. Activation of NRF2 by p62 and proteasome reduction in sphere-forming breast carcinoma cells. Oncotarget 2015;6(10):8167-84.
37. Mizuno T, Suzuki N, Makino H, Furui T, Morii E, Aoki H, et al. Cancer stem-like cells of ovarian clear cell carcinoma are enriched in the ALDH-high population associated with an accelerated scavenging system in reactive oxygen species. Gynecol Oncol 2014.
38. Linares V, Alonso V, Domingo JL. Oxidative stress as a mechanism underlying sulfasalazine-induced toxicity. Expert Opin Drug Saf 2011;10(2):253-63.
39. de la Fuente V, Federman N, Fustinana MS, Zalcman G, Romano A. Calcineurin phosphatase as a negative regulator of fear memory in hippocampus: control on nuclear factor-kappaB signaling in consolidation and reconsolidation. Hippocampus 2014;24(12):1549-61.
40. Dai L, Cao Y, Chen Y, Parsons C, Qin Z. Targeting xCT, a cystine-glutamate transporter induces apoptosis and tumor regression for KSHV/HIV-associated lymphoma. J Hematol Oncol 2014;7:30.
41. Robe PA, Martin DH, Nguyen-Khac MT, Artesi M, Deprez M, Albert A, et al. Early termination of ISRCTN45828668, a phase 1/2 prospective, randomized study of sulfasalazine for the treatment of progressing malignant gliomas in adults. BMC Cancer 2009;9:372.
42. Aurisicchio L, Mancini R, Ciliberto G. Cancer vaccination by electro-gene-transfer. Expert Rev Vaccines 2013;12(10):1127-37.
43. Rolla S, Nicolo C, Malinarich S, Orsini M, Forni G, Cavallo F, et al. Distinct and non-overlapping T cell receptor repertoires expanded by DNA vaccination in wild-type and HER-2 transgenic BALB/c mice. J Immunol 2006;177(11):7626-33.

44. Liao WT, Ye YP, Deng YJ, Bian XW, Ding YQ. Metastatic cancer stem cells: from the concept to therapeutics. Am J Stem Cells 2014;3(2):46-62.
45. Pardridge WM. The blood-brain barrier: bottleneck in brain drug development. NeuroRx 2005;2(1):3-14.
46. Srivastava MK, Sinha P, Clements VK, Rodriguez P, Ostrand-Rosenberg S. Myeloid-derived suppressor cells inhibit T-cell activation by depleting cystine and cysteine. Cancer research 2010;70(1):68-77.
47. McCullagh EA, Featherstone DE. Behavioral characterization of system xc- mutant mice. Behav Brain Res 2014;265:1-11.
48. Conklin KA. Chemotherapy-associated oxidative stress: impact on chemotherapeutic effectiveness. Integr Cancer Ther 2004;3(4):294-300.
49. Narang VS, Pauletti GM, Gout PW, Buckley DJ, Buckley AR. Sulfasalazine-induced reduction of glutathione levels in breast cancer cells: enhancement of growth-inhibitory activity of Doxorubicin. Chemotherapy 2007;53(3):210-7.
50. Wang F, Yang Y. Suppression of the xCT-CD44v antiporter system sensitizes triple-negative breast cancer cells to doxorubicin. Breast cancer research and treatment 2014;147(1):203-10.

Figure legends

Figure 1. xCT expression in breast CSC and tumors. (A) FACS analysis of xCT expression in TUBO cells and P1 to P3 tumorsphere passages over six independent experiments. (B) Representative density plots of xCT and Sca-1 expression on TUBO and tumorspheres. Numbers show the percentage of cells in each quadrant. (C) Representative immunofluorescence staining of xCT, Sca-1, OCT4 and Thy1.1 on tumorspheres. DAPI stains the nucleus. Scale bar 20 μm. (D) Representative density plots of xCT expression in TUBO cells stained with CD44 and CD24. (E) FACS analysis of xCT espression in HCC-1806, MDA-MB-231 and 4T1 cells and their derived tumorspheres over three independent experiments. **P*<0.05, ***P*<0.01, ****P*<0.001, Student's *t*-test. (F) Immunofluorescence of xCT expression (red) in normal breast, hyperplastic and IDC breast carcinoma. Scale bar 20 μm. (G) Percentage of xCT^+ samples in normal mammary gland and in TNBC, $Her2^+$ or ER/PR^+Her2^- breast cancer subtypes.

Figure 2. xCT regulates CSC self-renewal and the intracellular redox balance. (A, B) MTT assay of the cytotoxic effect exerted by scalar doses of SASP or by anti-xCT siRNAs on (A) TUBO and (B) tumorspheres. (C) Sphere generation ability relative to untreated cells of tumorspheres incubated with SASP. (D) Sphere generation ability of tumorspheres incubated with siRNAs to xCT, scrambled siRNA or not at all shown as tumorsphere number/10^3 plated cells. (E, F) FACS analysis of xCT and CSC marker expression in spheres 24 hours after transfection with siRNA to xCT or scrambled siRNA. (E) Gray histograms show xCT expression, open histograms show the background of negative control IgG stained cells from one representative experiment. (F) Relative expression (%) of xCT^+, $Sca\text{-}1^+$ and $CD44^{high}/CD24^{low}$ cells in tumorsphere-derived cells transfected with siRNAs to xCT (black bars) compared to cells transfected with scrambled siRNA (dashed line). (G, H) GSH (G) and ROS (H) levels in TUBO cells and their derived tumorspheres after either seeding in normal conditions, transfection with siRNAs to xCT or scrambled siRNA over three independent experiments. **P*<0.05, ***P*<0.01, ****P*<0.001, Student's *t*-test.

Figure 3. Vaccine-induced antibodies target CSC and affect their self-renewal and ROS flux. (A-C) TUBO-derived tumorsphere or (E-G) NIH/3T3 cell staining by antibodies present in the sera of BALB/c mice

vaccinated with pVAX1 or pVAX1-xCT, analyzed by FACS. Results are reported as (A, E) the mean fluorescence intensity (MFI) from 7 mice per group, (B, F) the percentage of positive cells, and (C, G) two representative dot plots. (D, H) Representative images of (D) TUBO-tumorspheres or (H) NIH/3T3 cells stained with IgG purified from sera of mice vaccinated with pVAX1 or pVAX1-xCT. Scale bar 20 μM. (I) Sphere generating ability of tumorspheres incubated for 5 days with IgG purified from the sera of mice vaccinated with pVAX1, pVAX1-xCT or not at all. Graph shows tumorsphere number/10^3 plated cells. FACS analysis of (L) CSC marker expression or (M) ROS production in tumorspheres incubated for 5 days with IgG purified from the sera of vaccinated mice or not at all, reported as (D) percentage of positive cells or of the (E) DCF MFI from four independent experiments. *P< 0.05, **P<0.01, Student's t-test.

Figure 4. Anti-xCT vaccination delays CSC-induced tumor growth *in vivo*.

BALB/c mice were s.c. challenged with tumorspheres derived from either (A-D) TUBO or (E-H) 4T1 cells and electroporated with (A, C, E, G) pVAX1 or (B, D, F, H) pVAX1-xCT plasmids when their tumor reached (A, B, E, F) 2 or (C, D, G, H) 4 mm mean diameter. Each black line depicts the growth of a single tumor. Data were cumulated from three independent and concordant experiments. Statistically significant differences in mean time required for pVAX1-xCT group and pVAX1 group tumors to reach 4, 6, 8 or 10 mm mean diameter are indicated by dashed gray lines. (I, L) Analysis of (I) the percentage of Aldefluor$^+$ cells in tumors explanted from vaccinated mice challenged s.c. with TUBO-derived tumorspheres and (L) number of tumorspheres generated *in vitro* by cells from the same tumors. *P<0.05, **P<0.01.

Figure 5. Anti-xCT vaccination reduces CSC-generated lung metastasis formation. (A-B and E-H) BALB/c and (C, D) BALB-μIgKO mice were vaccinated with either pVAX1 or pVAX1-xCT plasmids (A, C, E) before tumorspheres injection or (G) when mice had 2 mm mean diameter tumor. (A, C, E, G) Number of lung metastases in mice challenged (A, C) i.v. with TUBO- or (E, G) s.c. with 4T1-derived tumorspheres and enumerated (A, C) 20 days later or (E,G) when the primary tumor reached 10 mm mean diameter. (B, D, F, H) representative images of lung metastases after H&E staining **P<0.01, ***P<0.001, Student's t-test.

Figure 6. Anti-xCT vaccination enhances the effect of doxorubicin *in vivo*. (A, B) MTT assay of the cytotoxic effect exerted by incubation with scalar doses of doxorubicin in (A) TUBO and (B) tumorspheres. (C) Number of lung metastases in mice challenged i.v. with TUBO-derived tumorspheres and either vaccinated or not with pVAX1 and pVAX1-xCT plasmids alone or in combination with doxorubicin administration. (D-F) Tumor growth curves of BALB/c mice s.c. injected with TUBO derived tumorspheres and treated with doxorubicin in combination with (E) pVAX1 or (F) pVAX1-xCT vaccination when their tumors reached 2 mm mean diameter. Treatments were repeated the week later. Each black line depicts the growth of a single tumor. Student's *t*-test. **P*<0.05, ***P*<0.01, ****P*<0.001, Student's *t*-test.

Figure 1

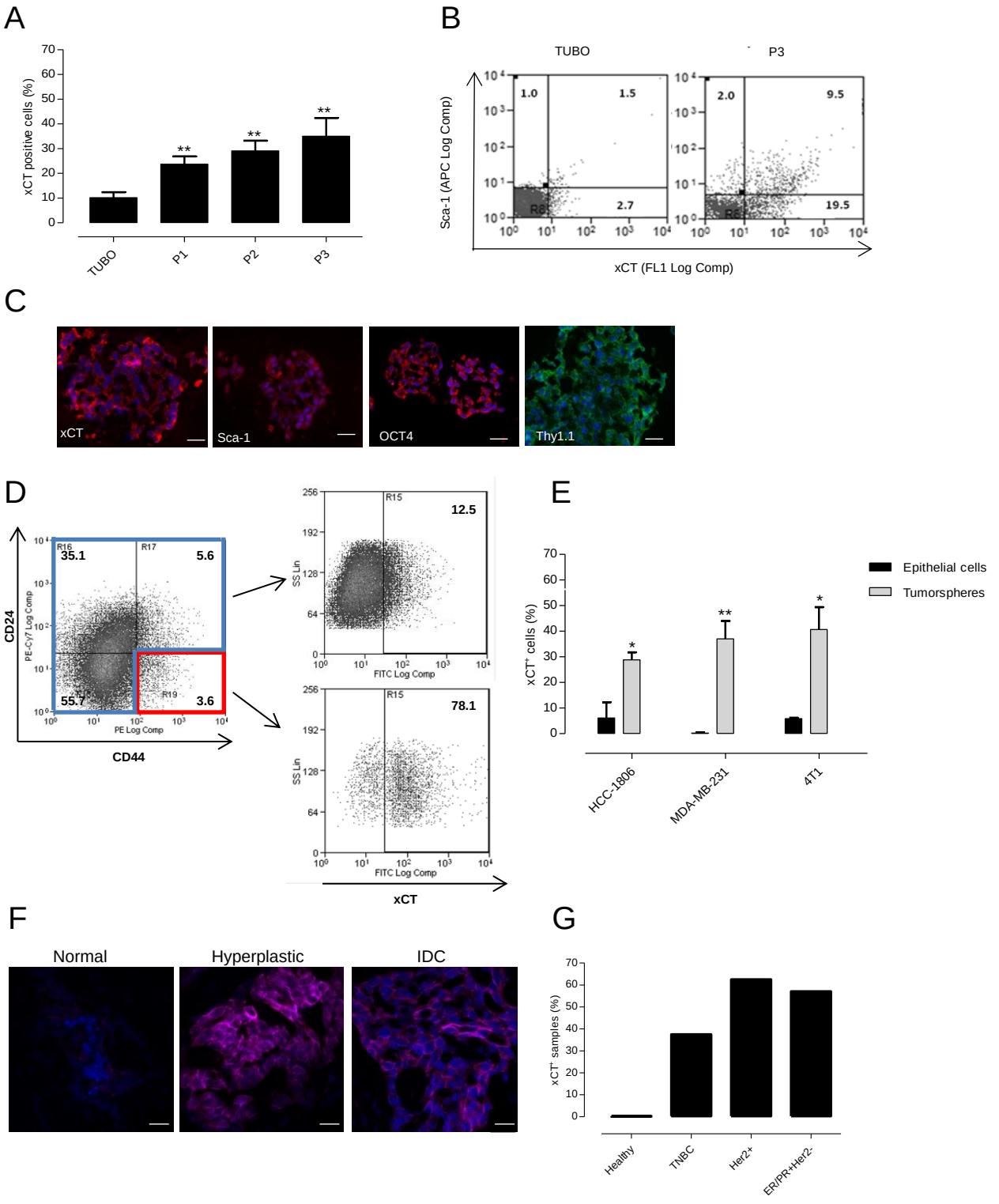
A
xCT positive cells (%)
TUBO
P1
P2
P3
B
TUBO
P3
Sca-1 (APC Log Comp)
xCT (FL1 Log Comp)
1.0
1.5
2.7
2.0
9.5
19.5
C
xCT
Sca-1
OCT4
Thy1.1
D
CD24
CD44
PE-Cy7 Log Comp
PE Log Comp
35.1
5.6
55.7
3.6
SS Lin
FITC Log Comp
12.5
78.1
xCT
E
xCT+ cells (%)
Epithelial cells
Tumorspheres
HCC-1806
MDA-MB-231
4T1
F
Normal
Hyperplastic
IDC
G
xCT+ samples (%)
Healthy
TNBC
Her2+
ER/PR+Her2-

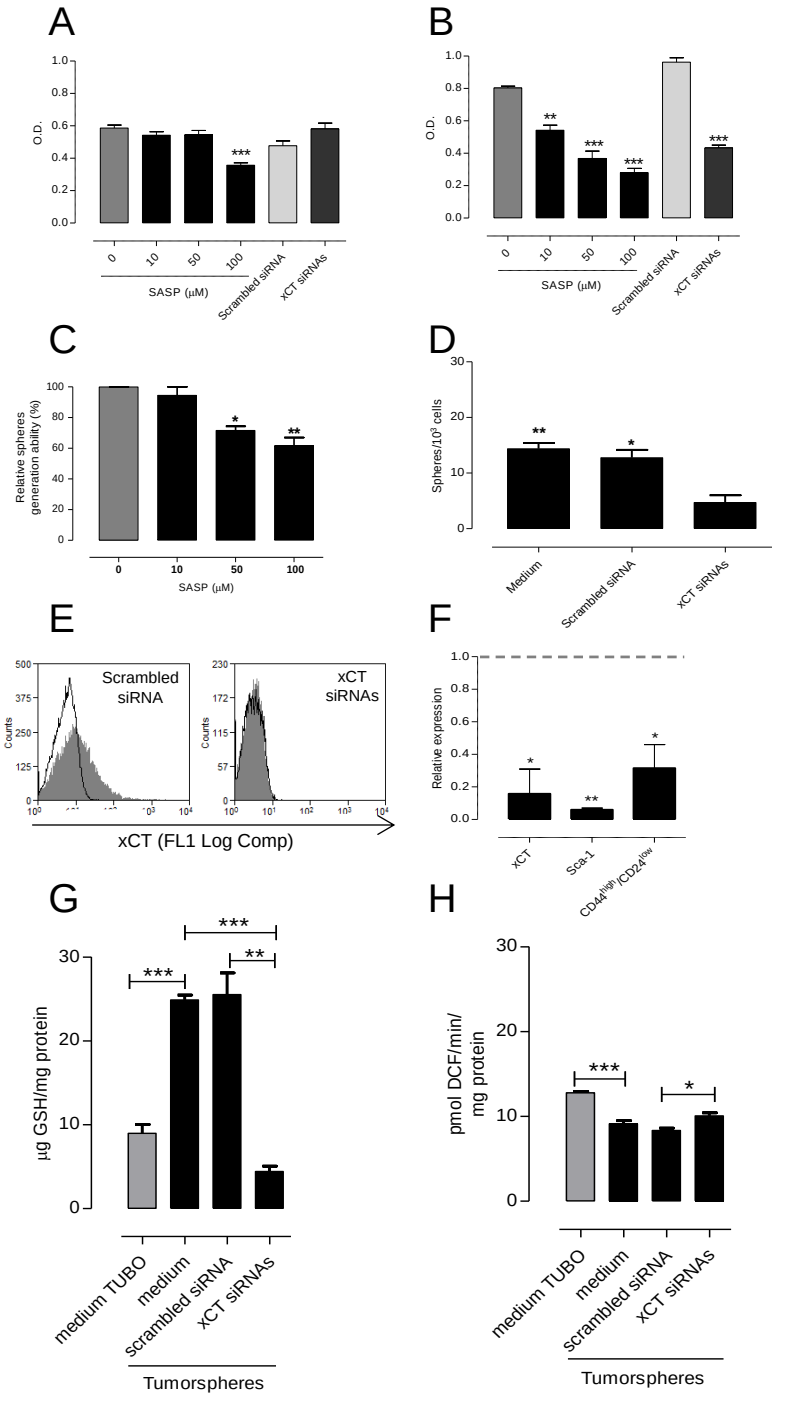
A
O.D.
SASP (μM)
Scrambled siRNA
xCT siRNAs
B
O.D.
SASP (μM)
Scrambled siRNA
xCT siRNAs
C
Relative spheres generation ability (%)
SASP (μM)
D
Spheres/10³ cells
Medium
Scrambled siRNA
xCT siRNAs
E
Scrambled siRNA
xCT siRNAs
Counts
xCT (FL1 Log Comp)
F
Relative expression
xCT
Sca-1
CD44high/CD24low
G
μg GSH/mg protein
medium TUBO
medium
scrambled siRNA
xCT siRNAs
Tumorspheres
H
pmol DCF/min/mg protein
medium TUBO
medium
scrambled siRNA
xCT siRNAs
Tumorspheres

Figure 3

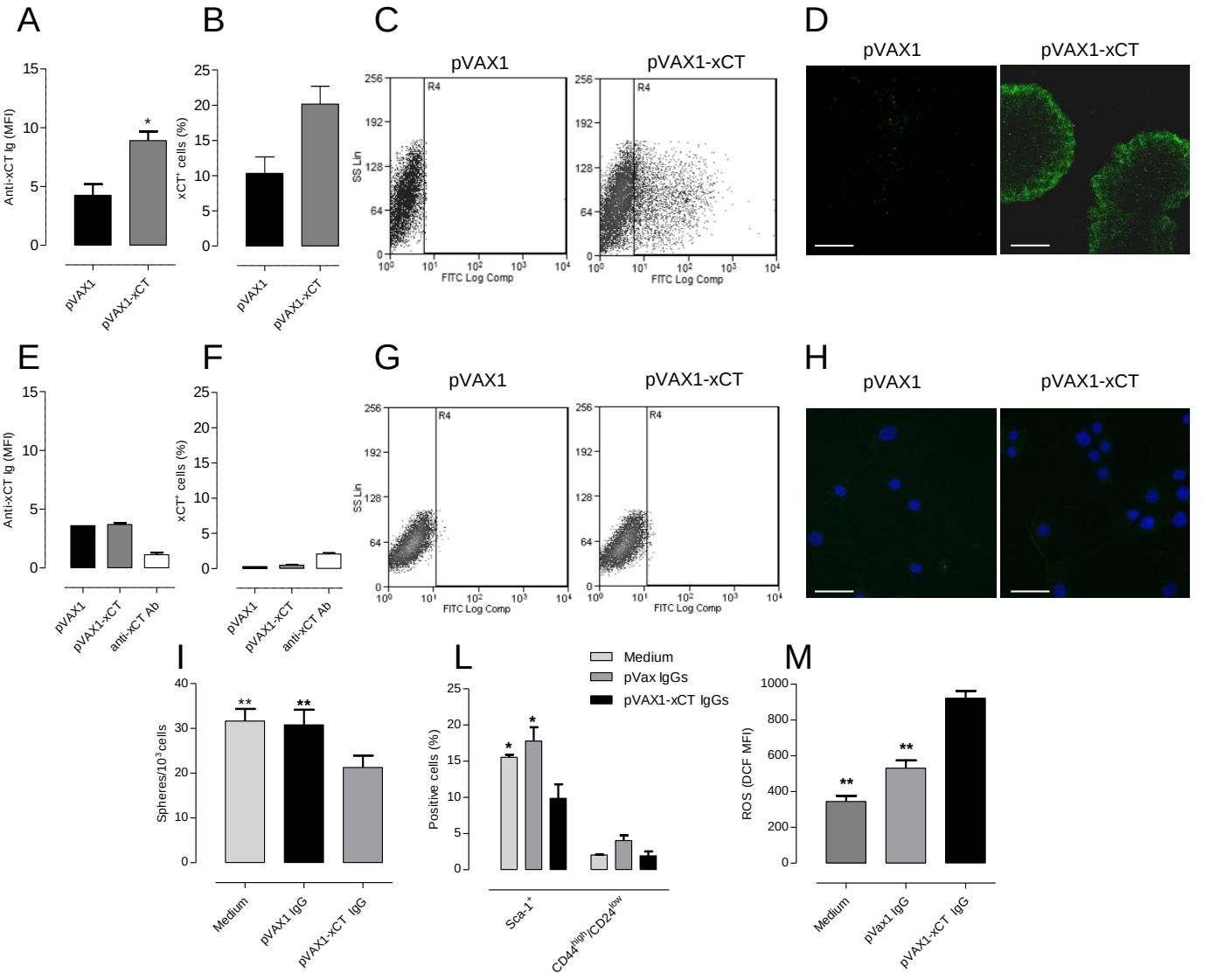
A
B
C
D
pVAX1
pVAX1-xCT
Anti-xCT Ig (MFI)
xCT+ cells (%)
SS Lin
FITC Log Comp
R4
E
F
G
H
anti-xCT Ab
I
L
M
Medium
pVax IgGs
pVAX1-xCT IgGs
Spheres/10³cells
Positive cells (%)
ROS (DCF MFI)
pVax1 IgG
pVAX1-xCT IgG
Sca-1+
CD44high/CD24low

Figure 4

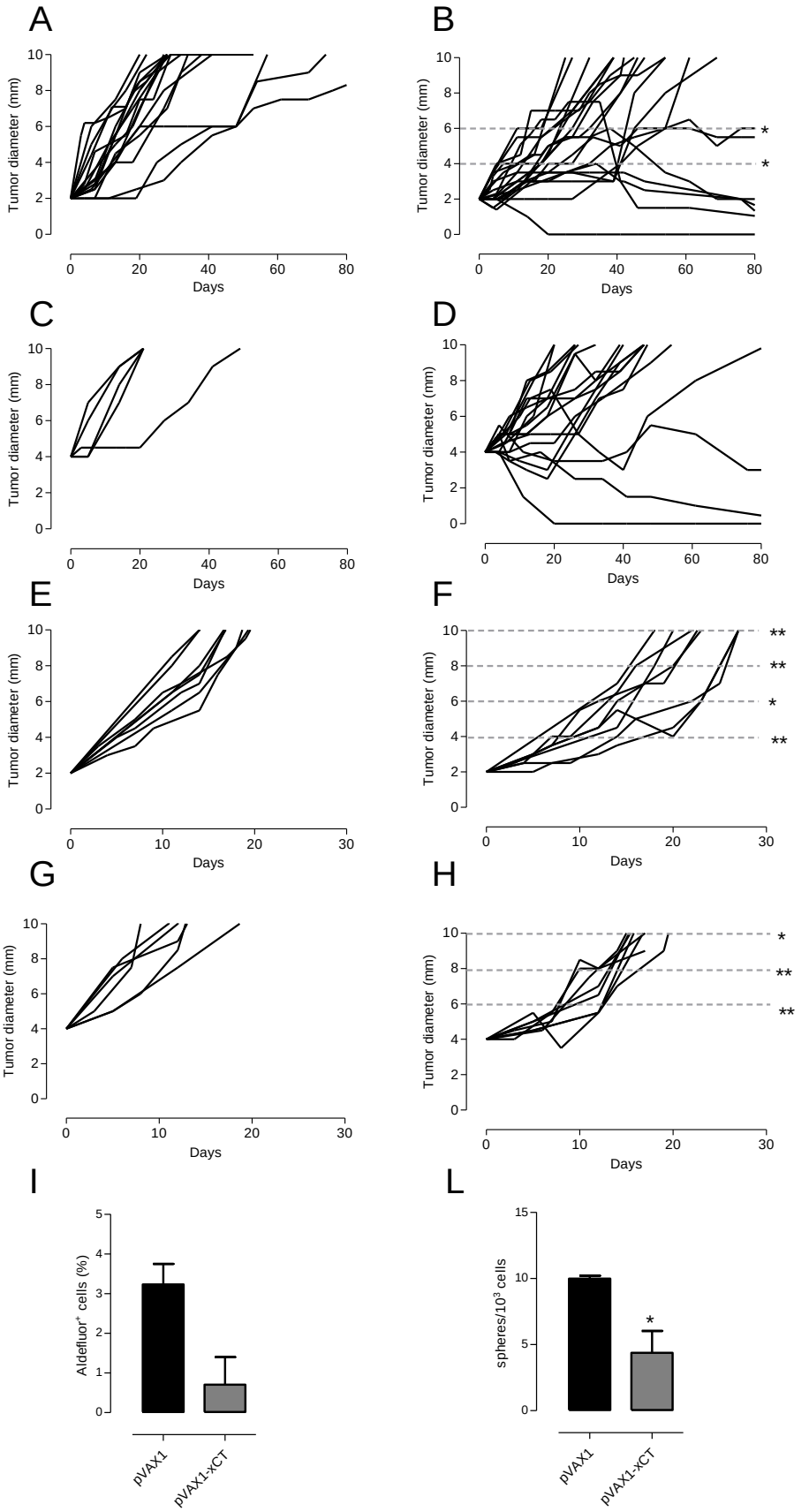
A
B
C
D
E
F
G
H
I
L
Tumor diameter (mm)
Days
*
**
Aldefluor+ cells (%)
sphere/10^3 cells
pVAX1
pVAX1-xCT

Figure 5

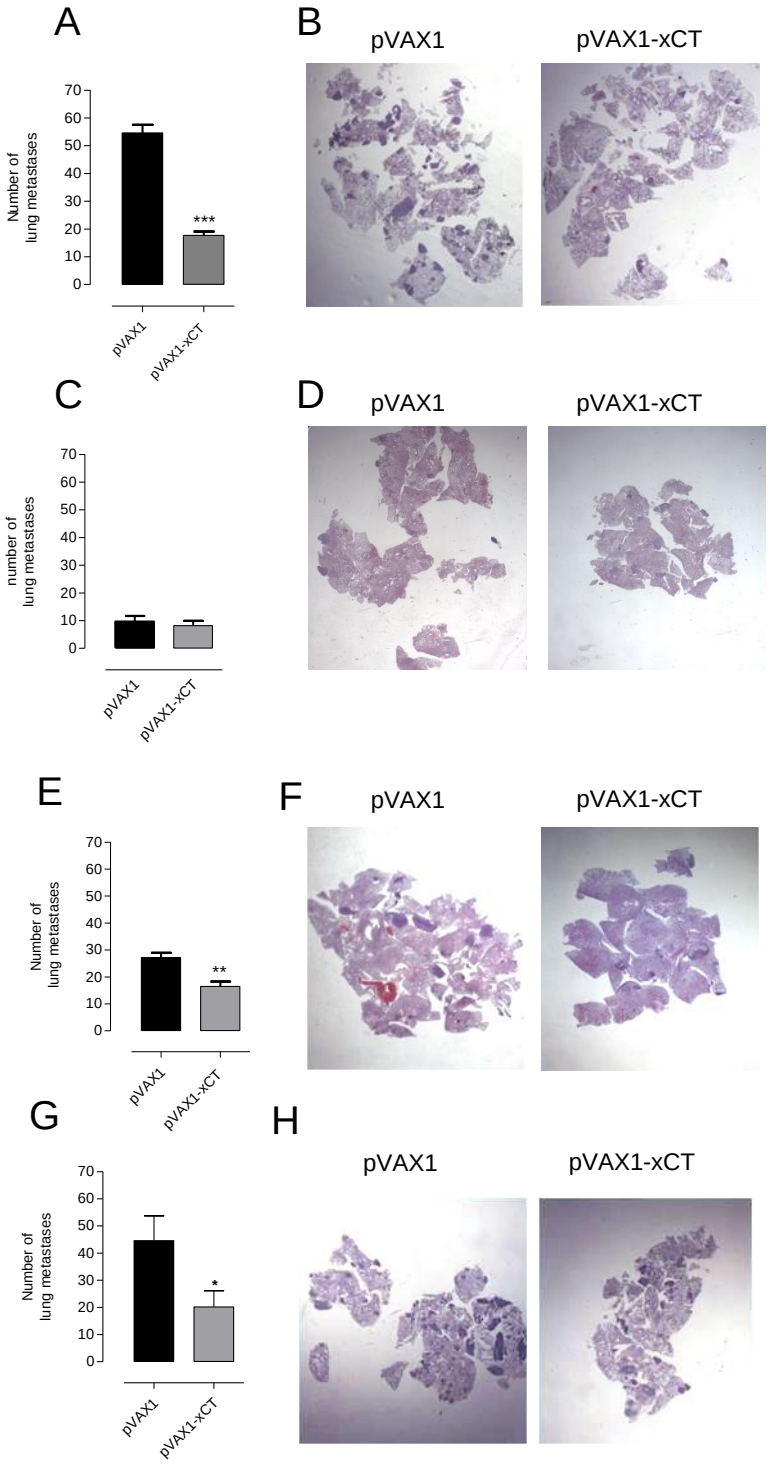
A
B
pVAX1
pVAX1-xCT
Number of lung metastases
70
60
50
40
30
20
10
0
***
pVAX1
pVAX1-xCT
C
D
pVAX1
pVAX1-xCT
number of lung metastases
70
60
50
40
30
20
10
0
pVAX1
pVAX1-xCT
E
F
pVAX1
pVAX1-xCT
Number of lung metastases
70
60
50
40
30
20
10
0
**
pVAX1
pVAX1-xCT
G
H
pVAX1
pVAX1-xCT
Number of lung metastases
70
60
50
40
30
20
10
0
*
pVAX1
pVAX1-xCT

Figure 6

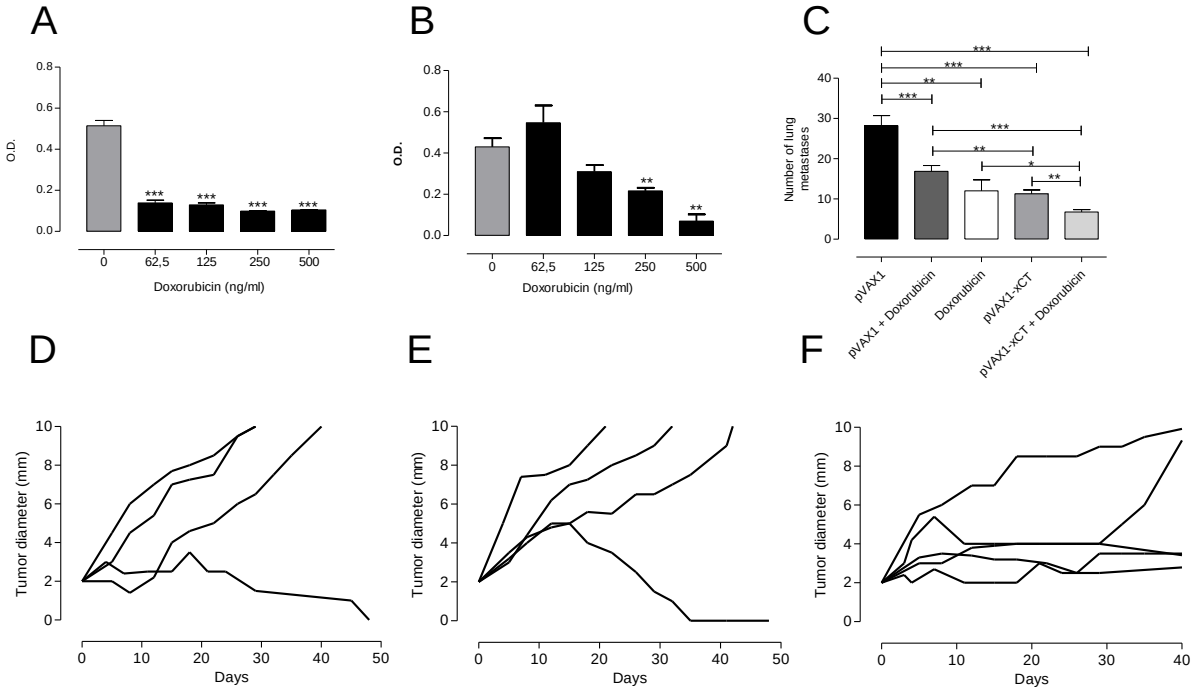
A
O.D.
0.8
0.6
0.4
0.2
0.0
***
***
***
***
0
62,5
125
250
500
Doxorubicin (ng/ml)
B
O.D.
0.8
0.6
0.4
0.2
0.0
**
**
0
62,5
125
250
500
Doxorubicin (ng/ml)
C
Number of lung metastases
40
30
20
10
0
***
***
**
***
***
**
*
**
pVAX1
pVAX1 + Doxorubicin
Doxorubicin
pVAX1-xCT
pVAX1-xCT + Doxorubicin
D
Tumor diameter (mm)
10
8
6
4
2
0
0
10
20
30
40
50
Days
E
Tumor diameter (mm)
10
8
6
4
2
0
0
10
20
30
40
50
Days
F
Tumor diameter (mm)
10
8
6
4
2
0
0
10
20
30
40
Days